JOURNAL OF GEOPHYSICAL RESEARCH, VOL. 110, C03018, doi:10.1029/2004JC002556, 2005

Short-timescale thermohaline variability and residual circulation in the central segment of the coastal upwelling system of the Ría de Vigo (northwest Spain) during four contrasting periods

S. Piedracoba
Universidade de Vigo, Vigo, Spain

X. A. Álvarez-Salgado
Instituto de Investigaciónes Mariñas, Consejo Superior de Investigaciones Científicas, Vigo, Spain

G. Rosón and J. L. Herrera
Universidade de Vigo, Vigo, Spain

Received 25 June 2004; revised 10 December 2004; accepted 19 January 2005; published 17 March 2005.

[1] Sixteen hydrographic surveys were carried out in the middle segment of the Ría de Vigo (northwest Spain) at 3- to 4-day intervals during February, April, July, and September 2002 (four surveys per period). Simultaneously, an acoustic Doppler current profiler (ADCP) mooring recorded the velocity profile. Combination of direct current measurements with the output of an inverse model based on the time course of the distributions of salinity and temperature allowed an objective analysis of the effect of the meteorological forces on the hydrodynamics of the Ría. Remote shelf winds explained more than 65% of the variability of the subtidal circulation, which responded immediately to this forcing (lag time, <2 days). Shelf winds created a simple two-layered circulation pattern, with a surface outgoing current under northerly winds and a surface ingoing current under southerly winds. A three-layered circulation developed during the transitions from northerly to southerly winds and vice versa. At the same time, an empirical orthogonal function (EOF) analysis demonstrated the lack of contribution of local winds to the subtidal dynamics of the ría. Continental runoff and heat exchange with the atmosphere explained less than 5% and 25% of the variability observed in the subtidal circulation of the Ría de Vigo.

Citation: Piedracoba, S., X. A. Álvarez-Salgado, G. Rosón, and J. L. Herrera (2005), Short-timescale thermohaline variability and residual circulation in the central segment of the coastal upwelling system of the Ría de Vigo (northwest Spain) during four contrasting periods, *J. Geophys. Res.*, *110*, C03018, doi:10.1029/2004JC002556.

1. Introduction

[2] Coastal embayments and estuaries respond to a variety of forcing mechanisms over a wide range of timescales [*Wong and Moses-Hall*, 1998]. Subtidal motion ultimately determines the long-term transport of suspended and dissolved materials, even though the semidiurnal or diurnal tidal motions are often the most energetic mechanisms operating in estuaries. Regarding subtidal motion, the density-induced gravitational circulation was the first to attract extensive research [*Pritchard*, 1952, 1956]. During the 1960s and 1970s, the two-layered gravitational circulation was established as the basic residual flow pattern associated with partially mixed estuaries.

[3] The importance of the atmospheric forcing for the subtidal variability was not fully recognized until the late 1970s, when *Carter et al.* [1979] reviewed the dynamics of motion in estuaries made by U.S. researchers during the period 1975–1978. This review highlighted that wind-induced fluctuations dominated the subtidal circulation of the Providence River [*Weisberg and Sturges*, 1976], the west passage of Narragansett Bay [*Weisberg*, 1976] or the Chesapeake Bay [*Wang and Elliott*, 1978]. Especially relevant was the paper by *Elliott* [1978] showing that 25% of the total variability of the residual currents in the Potomac Estuary was associated with remote winds from the adjacent shelf. The scientific interest on the wind-induced subtidal variability increased during the 1980s, with process-orientated studies conducted in estuaries such as San Francisco Bay [*Walters*, 1982], Delaware Bay [*Wong and Garvine*, 1984], and Mobile Bay [*Schroeder and Wiseman*, 1986] or some coastal lagoons with restricted communication with the ocean [e.g., *Wong and Wilson*, 1984]. Results from the above-mentioned studies revealed that the remote atmospheric forcing could produce subtidal variability in estuaries and coastal inlets by the impingement of coastal sea level fluctuations at the mouth of the estuary [*Wong and Moses-Hall*, 1998].

0148-0227/05/2004JC002556

[4] The Rías Baixas (northwest Spain) are four large (>2.5 km^3) and V-shaped coastal inlets, freely connected with the adjacent shelf. The rías produce annually more than 250,000 tons of mussels, which represent 25% of the world production [*Figueiras et al.*, 2002]. The nutrients necessary to support this culture are supplied by upwelled Eastern North Atlantic Central Water (ENACW), which eventually enters the rías [*Fraga*, 1981; *Rosón et al.*, 1997; *Álvarez-Salgado et al.*, 2000]. The western coast of the Iberian Peninsula is located at the boundary between the temperate and subpolar regimes of the coastal upwelling system of the Eastern North Atlantic, where upwelling-favorable northerly winds predominate from March–April to September–October in response to the seasonal migration of the Azores High. On the contrary, downwelling-favorable southerly winds prevail the rest of the year [*Wooster et al.*, 1976; *Bakun and Nelson*, 1991]. Warm and salty surface waters of subtropical origin pile on the shelf during downwelling events [*Haynes and Barton*, 1990, 1991]. However, this pattern explains <20% of the variability observed, whereas >70% concentrates at frequencies <30 days [*Nogueira et al.*, 1997].

[5] The recognized importance of coastal upwelling for the productivity of the rías focused the research during the 1990s on the effect of remote shelf winds on the hydrography of these coastal inlets at the timescale of an upwelling episode, 1–2 weeks [*Álvarez-Salgado et al.*, 1993]. Inverse modeling of thermohaline data collected with a one-half-week periodicity has been a useful tool to study the coupling between the wind blowing in the adjacent shelf and the subtidal circulation of the Ría de Arousa [*Rosón et al.*, 1997], Ría de Vigo [*Álvarez-Salgado et al.*, 2000; *Gilcoto et al.*, 2001] and Ría de Pontevedra [*Pardo et al.*, 2001]. These studies concluded that shelf winds were mainly responsible for the changes observed in the hydrography of the rías and that these changes were compatible with the assumption of a two-layered residual circulation pattern driven by shelf winds.

[6] A new tool has been recently introduced for the study of the remote wind-induced circulation of the rías: *Torres-López et al.* [2001] and *Souto et al.* [2001, 2003] applied the GHER (GeoHydrodynamics and Environment Research) and HANSOM (HAmburg Shelf Ocean Model) numerical models, respectively. They compared simulated with experimental data to conclude that the typical estuarine two-layered circulation pattern of the inner and middle Ría de Vigo overlaps with the alongshore circulation of the ría, which results from the interaction of shelf winds and the intricate topography of the coast. Thus a three-dimensional (3-D) residual circulation pattern has been proposed for the outer part of the ría.

[7] Despite the effort to understand the dynamics of the Rías Baixas, and particularly the Ría de Vigo, direct current measurements are scarce, with a restricted spatial and temporal coverage. *Álvarez-Salgado et al.* [1998] described an abnormal three-layered circulation pattern during a 1-day sampling in the middle Ría de Vigo in September 1991. *Gilcoto et al.* [2001] showed the coupling between the measured surface circulation of the middle ría and shelf winds during 20 days in September 1990. Finally, *Míguez et al.* [2001] and *Souto et al.* [2003] focused on the relationship between the residual currents at the northern and southern mouths of the outer Ría de Vigo and the winds blowing over the shelf. They were able to compute lag times ranging from 0 to 1 days at both mouths. However, until now it was unknown what is the relative importance of the different forcing to the residual circulation, what is the lag time of the water column response to the dominant agent forcing in a central segment of the ría, and in what conditions can be developed a scheme of circulation in three layers.

[8] With the aim of amending the lack of repeated current meter records under contrasting atmospheric and hydrographic conditions, an intensive program was conducted in the coastal upwelling system of the Ría de Vigo during 2002. Northerly and southerly wind conditions of variable intensity, as well as water column stratification (thermal and haline) and mixing conditions, were captured. In addition, direct current meter data were combined with a 2-D inverse model to provide complementary views of the residual circulation of the ría. For the first time, the vertical structure of the residual circulation of the middle ría will be resolved for a wide variety of atmospheric and hydrographic conditions, focusing on (1) the quantitative assessment of the relative importance of the different external forces acting on the system (remote and local winds, continental runoff, and heat exchange with the atmosphere) and (2) the lag time of the water column response in a well-protected site (15 km inshore of the shelf), compared with the outer ría (directly exposed to shelf winds). The contrasting conditions for (3) the development of the two-layered or the three-layered circulation patterns observed in the middle ría and (4) the depth of the level of no motion (LNM) separating layers flowing in opposite directions, will also be described. Finally, (5) the asymmetry in the response of the central segment of the Ría de Vigo to shelf winds will be examined on the basis of the differences observed in the salinity and temperature of a transverse hydrographic section. The results will be discussed in the wider context of the response of estuaries and coastal inlets to remote and local forcing agents.

2. Materials and Methods

[9] Sixteen surveys were carried out aboard R/V *Mytilus* during four contrasting periods in 2002 (four surveys per period). Every survey, a CTD SBE-25 was dipped at five selected stations along a transect transversal to the main axis of the embayment, from Cabo de Mar to Punta Borneira (Figure 1). An acoustic Doppler current profiler (ADCP) was moored at station R00, in 40 m water, to obtain a continuous record of the velocity profile during the four periods. In addition, a series of conductivity-temperature-depth (CTD) profiles along the main axis of the ría, from San Simon Bay to station R00, collected during 61 surveys to the Ría de Vigo between 1990 and 1997 were also used to complement the hydrographic data collected during 2002.

2.1. Measured Variables

[10] Current velocity profiles were measured with an Aandera DCM12 at the central station R00 (42°14.071′N

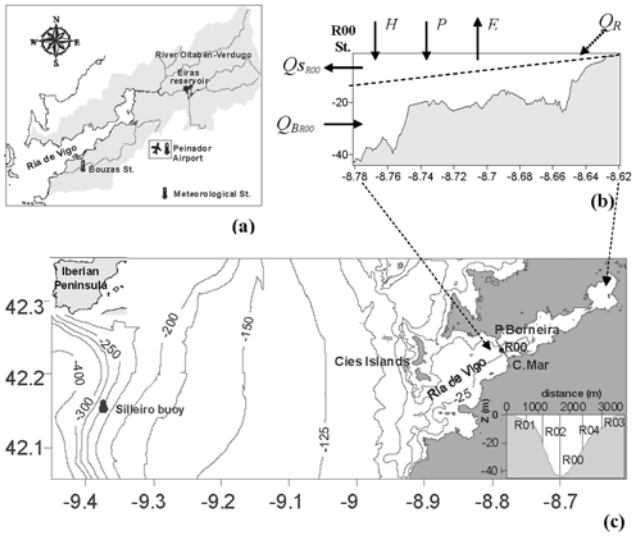

Figure 1. (a) Map of the Ría de Vigo showing the land-based meteorological stations of Bouzas and Peinador and the Eiras reservoir. (b) Section along the main channel of the Ría de Vigo showing the study volume used in the inverse box model application, with surface and bottom layer. The outer limit is the section between Cabo de Mar and Punta Borneira. Q_R, river discharge; E, evaporation rate; P, precipitation; H, atmospheric heat flux; Q_S and Q_B, the surface and bottom horizontal advective fluxes measured at the outer boundary. (c) Bathymetry of the Ría de Vigo and the adjacent shelf showing the meteorological station off Cape Silleiro and a detailed cross section between Cabo de Mar and Punta Borneira including station R00, where the Aanderaa DCM12 Doppler current meter was moored.

and 8°47.208′W). The site was chosen because it has been proven suitable for evaluating the main processes that take place in the system due to changes in the external forcing factors [*Nogueira et al.*, 1997]. The mooring was deployed during 24 days in February, 10 days in April, 19 days in July, and 9 days in September 2002. The DCM12 Doppler Current Meter was deployed on the seabed, and the following parameters were recorded at 30-min intervals: (1) the current at the sea surface and five depths and (2) the water level and significant wave height ($H_{1/3}$). Cell size was 11 m, centered at 6.5, 13, 19.5, 26, and 32.5 m, corresponding to L1, L2, L3, L4, and L5, respectively.

[11] Other data used in this study were (3) local winds, from the ship-mounted meteorological station and the meteorological observatory of Bouzas, National Institute of Meteorology (Figure 1); (4) remote winds, from the Seawatch buoy of Puertos del Estado off Cape Silleiro, a representative site for winds blowing off the Ría de Vigo (J. L. Herrera et al., Spatial analysis of the wind field on the western coast of Galicia from accurate measurements, submitted to *Continental Shelf Research*, 2005); (5) daily precipitation rates, from the meteorological observatory of Peinador airport, National Institute of Meteorology (Figure 1); and (6) humidity, air temperature, and atmospheric pressure, from the meteorological observatory of Bouzas. A $A_{24}^2 A_{25}$ filter with a cutoff period of 30 hours was passed to the time series of winds and currents, to remove the variability at tidal or higher frequencies [*Godin*, 1972].

2.2. Variables Calculated From Collected Data

[12] Daily values of the offshore Ekman transport ($-Q_X$, $m^3\ s^{-1}\ km^{-1}$) were calculated from *Wooster et al.* [1976],

$$-Q_X = -\frac{\rho_{air} C_D |V| V_y}{\rho_{SW} f_C}, \tag{1}$$

where ρ_{air} is the density of air, 1.22 kg m^{-3} at 15°C. C_D is an empirical drag coefficient (dimensionless), 1.3×10^{-3} according to *Hidy* [1972]; f_C is the Coriolis parameter at 42° latitude; ρ_{SW} is the density of seawater, ~1025 kg m^{-3}; and V and Vy are the wind speed and the north component of wind speed recorded at the Seawatch buoy off Cape Silleiro.

[13] Continental runoff to the inner Ría de Vigo is a combination of regulated and natural flows. The Eiras reservoir controlled 42 ± 16% of the total flow of the River Oitavén-Verdugo during the study year 2002. Daily flows were provided by the company in charge of the management of urban waters. The natural component of the flow per unit area (Q_R/A, in 1 $m^{-2}\ d^{-1}$) was calculated according to the empirical equation of *Ríos et al.* [1992b] from the daily precipitation in the drainage basin, $P(n)$,

$$\frac{Q_R}{A} = \frac{1-k}{k-k^{30+1}} \sum_{n=1}^{30} P(n) k^n. \tag{2}$$

This equation accounted for the influence of precipitation during the 30 days before the study date. The retention constant k has a value of 0.75 for the 586 km^2 drainage basin of the Ría de Vigo [*Ríos et al.*, 1992b]. River discharge data were not filtered, as they came in the form of daily average values.

[14] Evaporation rates (E, mm d^{-1}) were calculated with the empirical equation of *Otto* [1975], based on the local wind velocity (W, m s^{-1}) and the vapor pressure at the sea surface (e_s, in mbar) and 2 m above the sea surface (e_z),

$$E = (0.26 + 0.077W)(e_s - e_z), \tag{3}$$

$$e_z = e_{T_S} \times \left(1 + 10^{-6} \times P_r \times \left(4.5 + 6 \times 10^{-3} \times T_A^2\right)\right) \times (1 - 0.000537 \times S) \times \frac{Hu}{100}, \tag{4}$$

$$e_s = e_{T_S} \times \left(1 + 10^{-6} \times P_r \times \left(4.5 + 6 \times 10^{-3} \times T_S^2\right)\right) \times (1 - 0.000537 \times S), \tag{5}$$

where S (in psu), T_A, and T_S (in °C) are the surface salinity and the air and water temperatures, P_r is the atmospheric pressure, Hu is the relative humidity, and e_{T_A} and e_{T_S} (in mbar) are the distilled water vapor pressure at T_A and T_S, which can be calculated for temperatures between −40° and 40°C with [*Gill*, 1982]

$$\log e_T = \frac{0.7859 + 0.03477 \times T}{1 + 0.00412 \times T}. \tag{6}$$

[15] Heat exchange with the atmosphere (H) was evaluated considering the balance of the following terms: irradi-

ation, conduction, back radiation, reflection, and heat lost by evaporation. Irradiation (I, cal cm^{-2} d^{-1}) was calculated with the equation developed by *Rosón et al.* [1997] for 42°N,

$$I = \left[3.19 + 11.15 \sin^2\left(\pi \frac{355 - J}{365}\right)\right] \times (50.417 - 4.474N), \tag{7}$$

where J is Julian day, from 1 (1 January) to 365 (31 December), and N is the cloudiness in oktas. Conduction (C, in cal cm^{-2} d^{-1}) was obtained with the empirical equation of *Otto* [1975] that depends on the temperature gradient between the sea surface (T_S, in °C) and the atmosphere (T_A), and on local wind speed (W, in m s^{-1}),

$$C = 24.88(0.38 + 0.114W)(T_S - T_A). \tag{8}$$

[16] The back radiation term (B, cal cm^{-2} d^{-1}) was estimated with the equation of *Laevastu* [1963],

$$B = (297 - 1.87T_S - 0.96H)(1 - 0.1N). \tag{9}$$

Heat lost by reflection (R) was assumed to represent 6% of irradiation at our latitudes [*Otto*, 1975]. Finally, evaporation also implies a loss of energy that was calculated multiplying the rate of evaporation E (in mm d^{-1}) by 58.7 cal cm^{-2} mm^{-1}. The total heat balance was

$$H = I - E - C - B - R. \tag{10}$$

2.3. Estimation of Water Flows With an Inverse Method

[17] The 2-D, nonsteady-state, salinity-temperature weighted box model successfully applied by *Álvarez-Salgado et al.* [2000] to the Ría de Vigo was used in this work. This box model is able to estimate the average water fluxes (horizontal and vertical advection), under the assumptions of volume, heat, and salt conservation. Horizontal advection fluxes were calculated for the volume of the ría delimited by the transect from Cabo de Mar to Punta Borneira between two consecutive surveys (Figure 1c).

[18] A system of three linear equations, conservation of water (11), salt (12), and heat (13), can be written for the study volume,

$$\overline{Q}_S = \overline{Q}_B + \overline{R}, \tag{11}$$

$$V\frac{\Delta S}{\Delta t} = \overline{Q}_B \cdot \overline{S}_B - \overline{Q}_S \cdot \overline{S}_S, \tag{12}$$

$$V\frac{\Delta T}{\Delta t} = \overline{Q}_B \cdot \overline{T}_B - \overline{Q}_S \cdot \overline{T}_S + \overline{R} \cdot \overline{T}_R + \overline{H}, \tag{13}$$

where $\overline{Q}_S$ and $\overline{Q}_B$ (m^3 s^{-1}) are the average residual surface and bottom horizontal fluxes across the outer boundary between two consecutive surveys. The boundary is divided into two layers (surface and bottom) flowing in opposite directions. The limit between the surface and bottom layer (level of no horizontal motion, LNM) was set at the pycnocline.

[19] $\overline{R}$ (m^3 s^{-1}) is the freshwater balance of continental runoff ($\overline{Q}_R$), precipitation ($\overline{P}$), and evaporation ($\overline{E}$). $\overline{T}_B$, $\overline{T}_S$, and $\overline{T}_R$ (°C) are the average temperature of the surface and bottom flows across the open boundary of the box and the river flow, respectively. $\overline{S}_B$ and $\overline{S}_S$ are the average salinity of the surface and bottom flows across the open boundary. V is the volume of the box. $\overline{H}$ (m^3 °C s^{-1}) is the average heat exchange with the atmosphere. $\Delta S/\Delta t$ and $\Delta T/\Delta t$ are the net rate of change in salinity and heat content (temperature) of the study volume between two consecutive surveys.

[20] Two sets of horizontal bottom convective flows are obtained from the equations of water (11) and salt conservation (12), $(\overline{Q}_B)_S$, and the equations of water (11) and heat conservation (13), $(\overline{Q}_B)_T$,

$$(\overline{Q}_B)_S = \frac{\overline{R}\overline{S}_S + V\dfrac{\Delta S}{\Delta t}}{\overline{S}_B - \overline{S}_S} \tag{14}$$

$$(\overline{Q}_B)_T = \frac{\overline{R}(\overline{T}_S - \overline{T}_R) + V\dfrac{\Delta T}{\Delta t} - H}{\overline{T}_B - \overline{T}_S}. \tag{15}$$

[21] A salinity-temperature weighted horizontal bottom flow, $\overline{Q}_B$, can be obtained,

$$\overline{Q}_B = (\overline{Q}_B)_S \overline{f} + (\overline{Q}_B)_T (1 - \overline{f}), \tag{16}$$

where the dimensionless factor, $\overline{f}$, that weights the contribution of salinity and temperature to the density gradient at the open boundary is calculated as

$$\overline{f} = \frac{(\overline{S}_B - \overline{S}_S)^2}{(\overline{S}_B - \overline{S}_S)^2 + (\overline{T}_B - \overline{T}_S)^2 / (\overline{\beta}/\overline{\alpha})^2}. \tag{17}$$

The coefficient $\overline{\beta}/\overline{\alpha}$ converted the temperature gradient into salinity units, where $\overline{\beta}$ and $\overline{\alpha}$ are the coefficients of haline contraction and thermal expansion, respectively.

[22] The robustness of the estimated fluxes is inversely proportional to the vertical gradients of salinity and temperature. This is the reason why the factor $\overline{f}$ was introduced to weight the relative contribution of the salt, $(\overline{Q}_B)_S$, and temperature, $(\overline{Q}_B)_T$, solutions to the optimum salt-heat weighted solution, $(\overline{Q}_B)_{S,T}$. During the winter months the value of $\overline{f}$ is close to 1.0. Therefore the optimum solution coincided with the solution obtained from the salt balance because the temperature gradient is quasi homogeneous; this is $|T_B - T_S| = 0$. In contrast, during the summer months the value of $\overline{f}$ is close to 0.0. Therefore the optimum solution coincided with the solution obtained from the heat balance because the salt gradient is quasi homogeneous, this is $|S_B - S_S| = 0$.

[23] Since $\Delta S/\Delta t$ and $\Delta T/\Delta t$ in the study volume were not measured, a set of historical data for the same volume collected during the period 1990–1997 were used to infer the salinity and temperature of the box from the salinity and

Table 1. Eigenvectors and Percentage of the Total Variability of the Time Series of Local (Bouzas) and Shelf (Cabo Silleiro) Winds and the Measured Subtidal Flow in the Surface (S) and Bottom (B) Layer of the Middle Segment of the Ría de Vigo (Station R00) for the Three Main Modes Obtained in EOF Analysis

	EOF Mode 1				EOF Mode 2				EOF Mode 3			
	February		July		February		July		February		July	
	S	B	S	B	S	B	S	B	S	B	S	B
Percent	95.2	86.9	97.1	87.8	3.4	12.4	2.9	12.2	1.3	0.7	0.1	0.1
Bouzas	−0.11	−0.09	−0.01	−0.01	−0.48	−0.07	0.02	−0.01	0.87	0.99	−1.0	1.0
Silleiro	−0.95	−0.67	−0.99	−0.81	0.32	0.74	−0.14	0.58	0.06	−0.01	0.01	−0.01
Measured	−0.30	0.74	−0.14	0.58	−0.82	0.67	0.99	0.81	−0.49	0.12	0.02	0.01

temperature of the open boundary. The following linear regressions were obtained:

$$\overline{S}_{RÍA} = -8(\pm 2) + 1.2(\pm 0.05)\overline{S}_{R00} - 0.006(\pm 0.001)\overline{R}_{R00}, \quad R^2 = 0.95, n = 61, p < 0.0001, \tag{18}$$

$$\overline{T}_{RÍA} = 1.028(\pm 0.003)\overline{T}_{R00}, \quad R^2 = 0.93, n = 61, p < 0.0001, \tag{19}$$

where $\overline{S}_{R00}$, $\overline{T}_{R00}$, and $\overline{R}_{R00}$ are the salinity, temperature, and hydrological balance at station R00 from the set of historical data. Therefore $\Delta S/\Delta t$ and $\Delta T/\Delta t$ in the inner ría were obtained from equations (18) and (19), using the thermohaline data recorded during the 2002 surveys in station R00. Equation (16) can be split in a steady-state term and a nonsteady-state term,

$$\left(\overline{Q}_B\right) = \left(\overline{Q}_B\right)_{SS} + \left(\overline{Q}_B\right)_{NSS}. \tag{20}$$

[24] Furthermore, the steady-state term, $\left(\overline{Q}_B\right)_{SS}$, can be divided in a hydrological term, $\left(\left(\overline{Q}_B\right)_{SS}\right)_H$, and a radiative term, $\left(\left(\overline{Q}_B\right)_{SS}\right)_R$,

$$\left(\left(\overline{Q}_B\right)_{SS}\right)_H = \frac{R\overline{S}_S}{\overline{S}_B - \overline{S}_S} f + \frac{\overline{R}\left(\overline{T}_S - \overline{T}_R\right)}{\left(\overline{T}_B - \overline{T}_S\right)}(1-f) \tag{21}$$

$$\left(\left(\overline{Q}_B\right)_{SS}\right)_R = -\frac{H}{\left(\overline{T}_B - \overline{T}_S\right)}(1-f). \tag{22}$$

2.4. Empirical Orthogonal Functions (EOF) Analysis of Local Winds

[25] An EOF analysis is a multivariate statistical technique that decomposes the total variability of a time series into a set of modes ordered by the percentage of the total variance that they explain. These modes are the orthogonal and uncorrelated eigenvectors of the complex covariance matrix of the time series, and the eigenvalue of each eigenvector is the percentage of the total variance explained by each mode [*Kundu and Allen*, 1976; *Kelly et al.*, 1988].

[26] An EOF analysis of the February and July 2002 time series of Silleiro and Bouzas winds and the surface (or bottom) flows at station R00 was preformed to study the relative influence of remote and local winds on the dynamics of the ría. The differences in roughness length between the remote (ocean based) and local (land based) meteorological stations were accounted [*Agsterberg and Wieringa*, 1989] by normalizing the friction between the two locations and using the method of *Wieringa* [1986] to interpolate the wind field originated from data taken at different locations.

2.5. Cross Correlation Between Shelf Winds and Residual Currents

[27] The cross-correlation coefficient is a statistical parameter that allows calculation of the correlation between two time series W(t) and V(t + τ) that are out of phase with a lag time τ. The curve shape $R(\tau)$ versus τ represents the variation of the correlation between the two time series depending on the lag time. This analysis was applied to the residual currents in the middle ría along the preferent direction (the main axis of the ría) and the North component of the wind recorded off Cape Silleiro during the four study periods.

3. Results

3.1. Local and Remote Winds

[28] The results of the EOF analyses of the time series of subtidal surface and bottom flows calculated from local winds, remote winds, and ADCP current measurements yielded similar results for February and July (Table 1). The analysis including the bottom flows calculated with the ADCP current meter produced two main modes that explained 87% and 12% of the total variability. The flows estimated from local winds do not contribute significantly to both eigenvectors. On the contrary, the flows estimated from shelf winds and the flows estimated with the ADCP current meter presented similar absolute values.

[29] When the surface flows are included in the analysis, there was only one dominant mode that explained 95% of the total variability. The flows estimated from local winds had again a small contribution to the eigenvector. However, the flows estimated from shelf winds yielded a coefficient larger than the flows estimated from surface ADCP measurements. This discrepancy probably arises from the lack of ADCP measurements in the top few meters, where the current velocities are larger. The small contribution of surface and bottom flows estimated from local winds to the main EOF modes analyses is interpreted as a nonsignificant influence of local winds to the residual dynamics of the ría.

[30] Since the EOF analyses revealed that only shelf winds have an influence on the subtidal circulation of the Ría de Vigo, the wind regime recorded at the Seawatch buoy off Cape Silleiro will be described for the winter, spring, summer, and autumn periods studied in 2002.

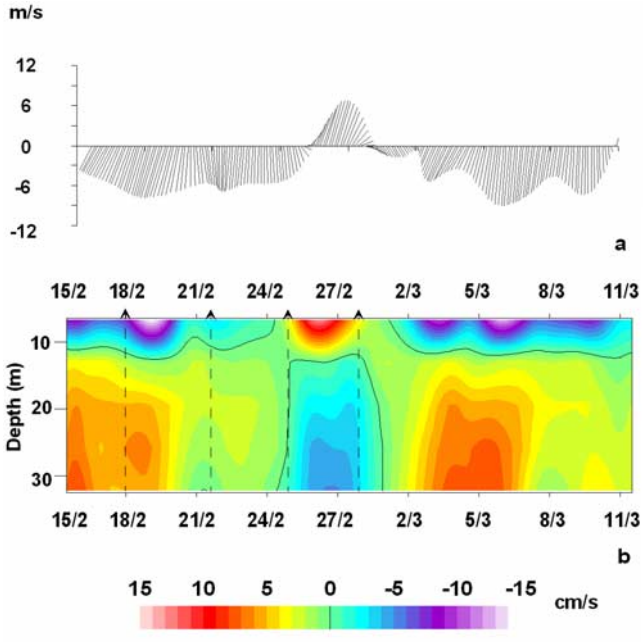

Figure 2. (a) Low-pass filtered wind velocity from the meteorological station off Cabo Silleiro during the winter period. (b) Time evolution of the low-frequency component (30-hour cutoff period) of the current velocity measured at station R00 along the direction perpendicular to the section between Cabo de Mar and Punta Borneira. The dotted lines indicate the hydrographic sampling dates. Positive values of V indicate an inflow, and negative values of V indicate an outflow. The solid black line represents the level of no motion, LNM (V = 0).

[31] Figure 2a shows the low-pass filtered fluctuations of shelf winds during February 2002, when two northerly wind episodes, which lasted about 1 week, separated by a short southerly wind event occurred. The intensity of the northerly winds ranged from -7 to -10 m s^{-1} during the first episode and from -6 to -9 m s^{-1} during the second episode. Southerly winds in between ranged from 6 to 9 m s^{-1}. During April 2002, northerly winds ranging from -3 to -6 m s^{-1} prevailed, but they persist for no longer than 3 days (Figure 3a). The wind speed reduced to near -1 m s^{-1} during the relaxation periods. During July 2002, northerly winds blew continuously but with a wide range of intensities (Figure 4a). Three periods can be defined: a first period, when northerly winds varied between -1 and -10 m s^{-1}; a second period of calm, with shelf winds intensities between 0 and -3 m s^{-1}; and a third period of vigorous northerly winds, with an average wind speed of -10 m s^{-1}. Finally, during September 2002, three periods can also be defined: a first period, when southeasterly winds decreased gradually from 6 to 3 m s^{-1}; a second period of transition from southerly to northerly winds; and a third period, when moderate northeasterly winds of less than -4 m s^{-1} blew over the shelf (Figure 5a).

3.2. Residual Currents

[32] The low-pass filtered subtidal fluctuations of the current are presented in Figures 2b, 3b, 4b, and 5b. The current vectors are projected along the preferred direction of water displacement: perpendicular to the transverse section between Cabo de Mar and Punta Borneira, as obtained from dispersion graphs. Positive values indicate inflow, whereas negative values indicate outflow.

[33] A two-layered estuarine circulation pattern, characteristic of partially mixed estuaries, was found during February 2002 (Figure 2b). The residual circulation was positive under the influence of northerly winds blowing on the shelf. When shelf winds changed to southerly, the circulation pattern reversed: An inflow was recorded through the surface layer and an outflow through the bottom layer. The level of no motion (LNM) separating the two layers was found between 11 and 13 m during this winter period. The cross-correlation coefficient between the residual current and the north component of shelf winds as a function of the lag time between them is presented in Figure 6a for the five ADCP layers. The curve shape $R(\tau)$ versus τ presented the maximum correlation, near 0.9, with a 0–0.1 day lag time for all layers, indicating an immediate response of the ría to the remote atmospheric forcing. Layer 1 (surface) was positively

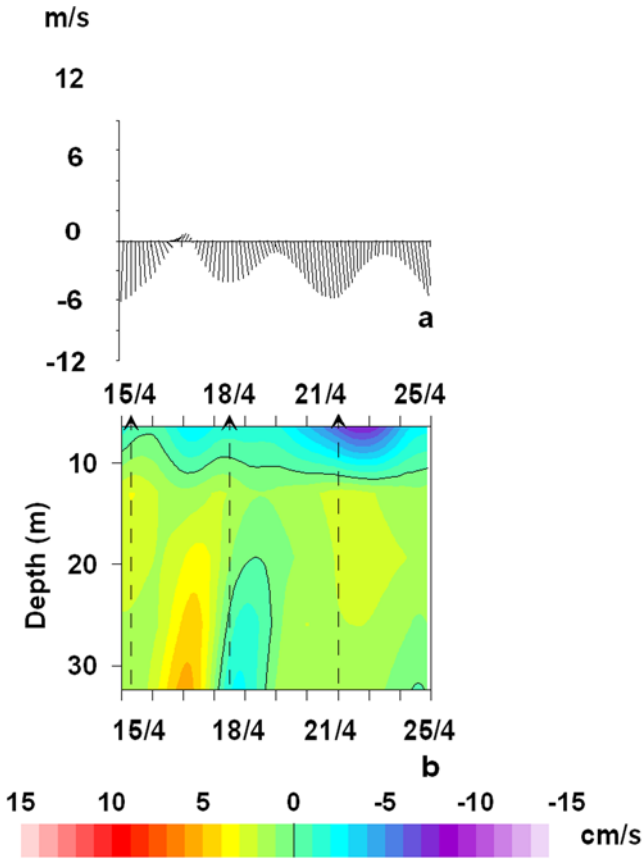

Figure 3. (a) Low-pass filtered wind velocity from the meteorological station off Cabo Silleiro during the spring period. (b) Time evolution of the low-frequency component (30-hour cutoff period) of the current velocity measured at station R00 along the direction perpendicular to the section between Cabo de Mar and Punta Borneira. The dotted lines indicate the hydrographic sampling dates. Positive values of V indicate an inflow, and negative values of V indicate an outflow. The solid black line represents the level of no motion, LNM (V = 0).

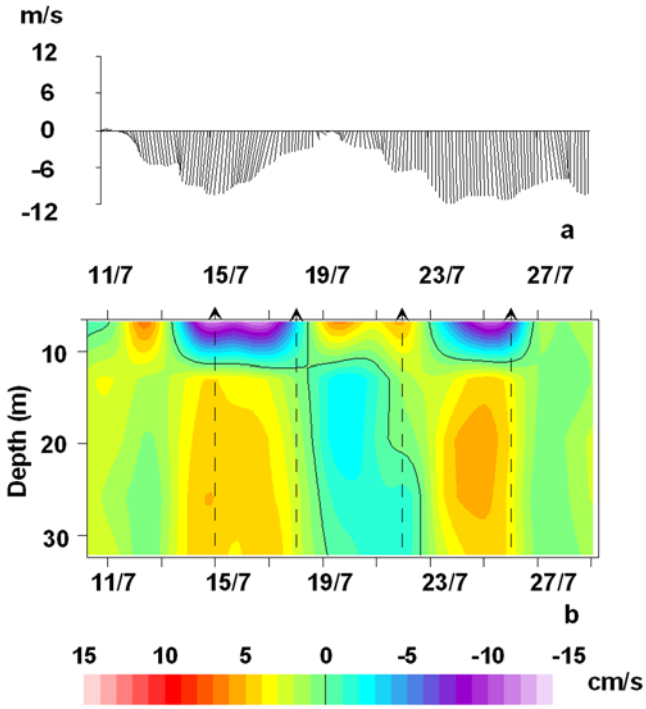

Figure 4. (a) Low-pass filtered wind velocity from the meteorological station off Cabo Silleiro during the summer period. (b) Time evolution of the low-frequency component (30-hour cutoff period) of the current velocity measured at station R00 along the direction perpendicular to the section between Cabo de Mar and Punta Borneira. The dotted lines indicate the hydrographic sampling dates. Positive values of V indicate an inflow, and negative values of V indicate an outflow. The solid black line represents the level of no motion, LNM (V = 0).

correlated with Wy. Therefore, northerly winds (Wy < 0) originated a surface outflow (V < 0). On the contrary, layers 2 to 5 showed a negative correlation with shelf winds.

[34] The characteristic two-layered circulation pattern was observed again in the low-pass filtered transversal current velocity profile at station R00 during April 2002 (Figure 3b). The LNM was at 10–11 m depth, except at the beginning of the study period when the surface layer was thinner. Especially remarkable was the transitional three-layered circulation pattern observed on 19 April, with outflow through the surface and bottom layers and inflow through the mid water column. This particular residual current distribution was found after a wind relaxation event. The water column responded to weak winds with weak residual currents, reaching a maximum outflow velocity of -8 cm s^{-1} and a maximum inflow of 5 cm s^{-1}. The scalar cross-correlation coefficient between residual current and shelf winds as a function of the lag time (Figure 6b) presented a maximum between 0 and 0.5 days for layers 1 and 2, and between 1.5 and 2 days for layers 3, 4, and 5. The coefficient was lower than 0.5 for layers 4 and 5, which contained the LNM when the three-layered distribution pattern arose. Again, the coefficient was positive for layer 1 and negative for layers 2 to 5. The relative weakness of shelf winds during the spring period was the reason behind the poor correlation coefficients.

[35] The low-pass filtered transversal current velocity profile at station R00 during July 2002 (Figure 4b) was characterized by a strong surface outflow reaching -12 cm s^{-1} during the first period of upwelling-favorable northerly winds. The second period corresponded to a profound relaxation of shelf winds, which produced a reversal of the residual circulation pattern; the surface inflow extended over the upper 12 m with a celerity of <7 cm s^{-1}, and the bottom outflow was lower than -3 cm s^{-1}. Finally, intense shelf northerly winds changed again the circulation pattern during the third period, with surface and bottom currents similar to the first period. The cross-correlation coefficient (Figure 6c) between the residual current and the north component of shelf winds was about -0.8 for layers 2 to 5, whereas for layer 1 it was just >0.6, because it included the LNM. The curve shape indicates that the correlation was independent of lag times ranging from 0 to -48 hours.

[36] During September 2002, the residual current pattern was initially negative in response to the dominant southerly winds blowing over the shelf. Maximum surface inflow currents of 10 cm s^{-1} and bottom outflow currents of -10 cm s^{-1} were recorded (Figure 5b). The LNM was deeper (17 m) than in the previous downwelling episodes of

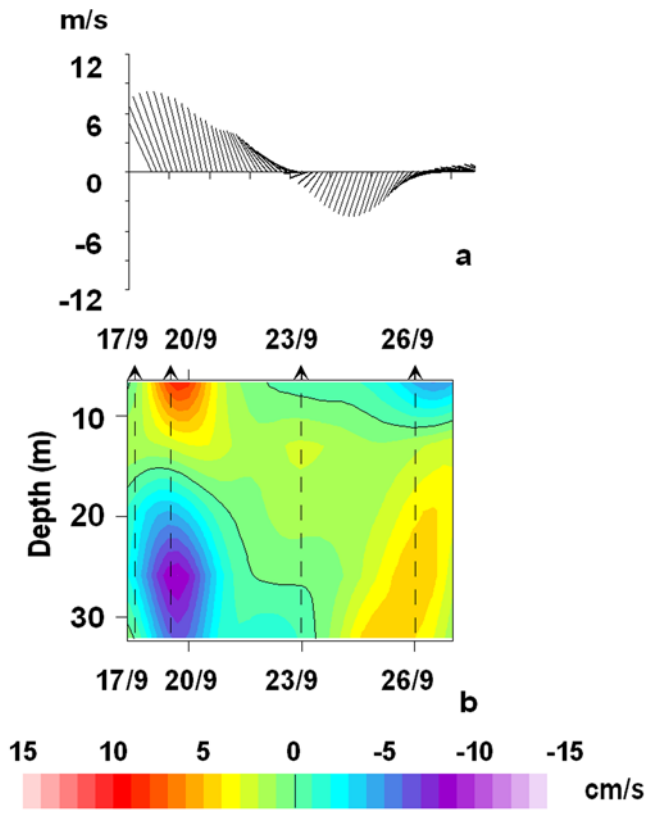

Figure 5. (a) Low-pass filtered wind velocity from the meteorological station off Cabo Silleiro during the autumn period. (b) Time evolution of the low-frequency component (30-hour cutoff period) of the current velocity measured at station R00 along the direction perpendicular to the section between Cabo de Mar and Punta Borneira. The dotted lines indicate the hydrographic sampling dates. Positive values of V indicate an inflow, and negative values of V indicate an outflow. The solid black line represents the level of no motion, LNM (V = 0).

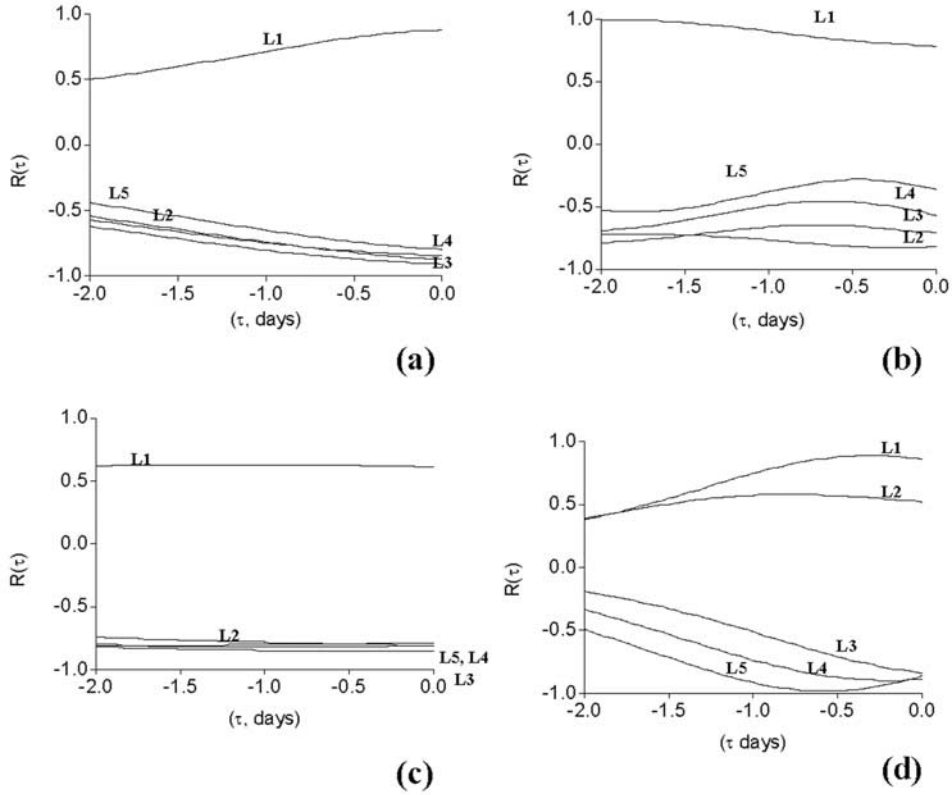

Figure 6. Cross correlation coefficients between the residual current in the middle Ría de Vigo (station R00) and the North component of shelf winds recorded at the Cabo Silleiro buoy as a function of the lag time between residual currents and winds for (a) winter, (b) spring, (c) summer and (d) autumn.

February and July 2002. In response to the relaxation of southerly winds, the reversal of the residual pattern persisted but current velocities diminished and the LNM deepened. During the transition from southerly to northerly shelf winds, on 23 September, the circulation evolved to a three-layered pattern, with outflow through the surface and bottom layers and inflow through the intermediate layer. The subsequent dominance of northerly winds re-established the two-layered positive circulation pattern, typical of upwelling-favorable winds, with an average velocity of about -5 cm s^{-1} in the surface layer and 5 cm s^{-1} in the bottom layer. The LNM was shallower ($\sim$10 m) than during the previous downwelling conditions. Finally, although shelf winds change again to southerly, the intensity was not enough to produce a reversal of the residual circulation pattern. The cross-correlation coefficient (Figure 6d) between residual currents and shelf winds was near 0.9 for all layers except 2 and 3, which contained the LNM. All layers exhibited the maximum correlation near 0.5 days, and the correlation diminished abruptly for lag times larger than 1 day. The correlation was positive for layers 1 and 2, and opposite for the rest indicating that southerly winds (Wy > 0) favored the entry of water through the upper layers 1 and 2, while the outflow was located in layers 3 to 5.

3.3. Thermohaline Variability

[37] A CTD probe was dipped at five hydrographic stations (R00 to R04) along the transect from Cabo de Mar to Punta Borneira (Figure 1). Completion of the transect took about 20 min. It was repeated on four dates in February (Figure 7), April (Figure 8), July (Figure 9), and September (Figure 10) with a periodicity of one-half week.

[38] During February 2002, a brief thermal inversion caused by winter cooling was observed. Heat exchange with the atmosphere (H) was negative (Figure 11a), although the loss of energy diminished from the beginning to the end of the study period. The hydrological balance ranged from 5 to 20 m^3 s^{-1}. The dominant northerly winds at the beginning of the study period caused the entry of very salty (>35.8) ENACW throughout the bottom layer of the ría (Figure 7a) that upwelled to the surface layer. Upwelling of ENACW produced a marked increase of salinity, especially in the northern side of the transverse section (Figure 7b). In response to the subsequent relaxation of shelf northerly winds, ENACW pulled back to the shelf and the bottom salinity decreased to 35.6 (Figure 7c). Finally, the dominant southerly winds from 25 February on produced a reversal of the residual circulation pattern, which piled the fresh water runoff in the surface layer ($S < 35.2$) and evacuated the bottom waters of the ría ($S = 35.4$) through the bottom outgoing current (Figure 7d). Since the thermal inversion maintained during the whole period (Figures 7e–7h), salinity controlled the hydrographic variability and the gravitational circulation.

[39] During April 2002, a marked haline stratification produced by continental runoff waters occurred at the beginning of the study period (Figure 8a). The halocline was situated at 10–15 m. On the contrary, temperature was

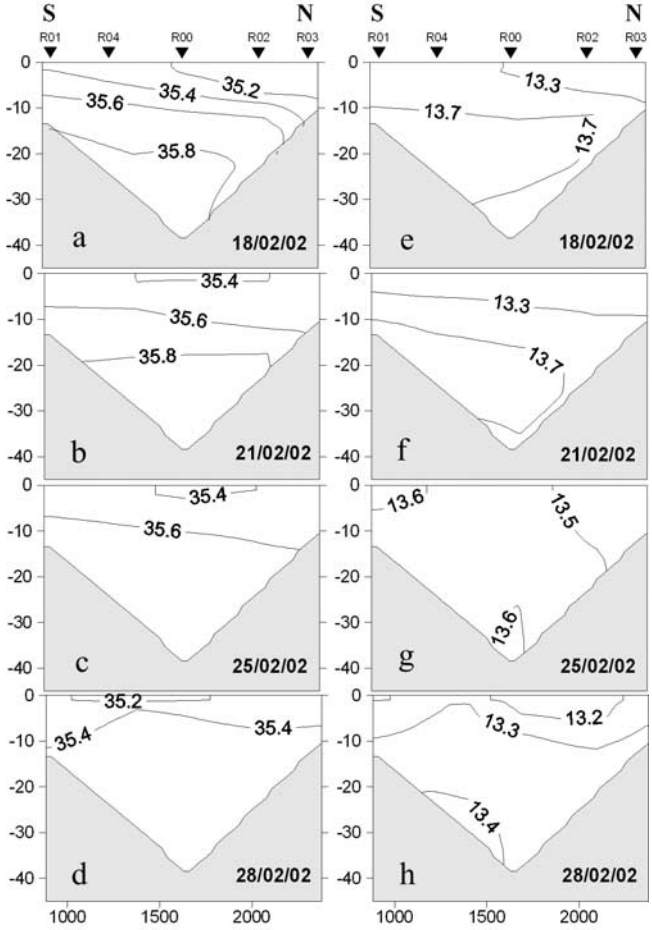

Figure 7. Contour plots of (a–d) salinity and (e–h) temperature along the section between Cabo de Mar and Punta Borneira from 18 to 28 February 2002.

homogeneously distributed, ranging from 13.5° to 13.7°C (Figure 8e). The thermal inversion observed in February 2002 had practically disappeared. Reduction of the fresh water flow (Figure 11b) produced a weakening of the haline stratification (Figure 8b). Surface salinity was not homogenous: Lower values were recorded in the northern side of the transect because of the Coriolis deflection to the right of continental runoff. At the bottom, salinity increased due to the entry of ENACW in response to the dominant northerly winds. A marked change in the distribution of temperature was observed on 18 April (Figure 11g); it can be observed how a weak surface thermocline was established (near 20 m depth) due to the differences between the colder oceanic water that was introduced into the ría through the bottom layers and the surface warmer fresh water. Finally, the increasing solar irradiation (Figure 11b) was able to produce a marked thermal stratification at the end of the study period. These are the appropriate conditions for the development of the spring bloom in the rías [*Nogueira et al.*, 1997].

[40] During July 2002, temperature rather than salinity gradients controlled the density distribution in the middle ría (Figure 9). Continental runoff was very low throughout the study period (<9 m^3 s^{-1}; Figure 11c). On 15 July, the salinity and temperature distributions showed the typical response of the water column to an upwelling event: The northern side of the transect was fresher (Figure 9a) and warmer (Figure 9e) than the southern side. The thermocline was at about 10 m depth. Despite the subsequent relaxation of shelf winds, the effect of coastal upwelling still remained in the water column 3 days later, when higher salinities (Figure 9b) and lower temperatures (Figure 9f) were recorded. The reversal of the circulation in response to the shelf winds calm (Figure 4) had a clear impact on the water column: Salinity was more homogenous and the halocline was difficult to distinguish (Figure 9c) while surface temperature increased and the maximum gradient was found over 20 m depth (Figure 9g). Shelf water tended to enter the ría through the surface layer and be forced to sink. This downwelling process was favored because river discharge was negligible. From 23 July onward, intense and persistent northerly winds changed again the circulation pattern. The reduced river discharge left the estuary by the surface layers, and saltier (Figure 9d) and colder water (Figure 9h) entered into the ría through the bottom layer.

[41] Finally, during September 2002, the freshwater flow was again very limited: from 5.7 to 14.5 m^3 s^{-1} (Figure 11d). The thermohaline structure found on 17 September corresponded with a typical autumn downwelling, with warm

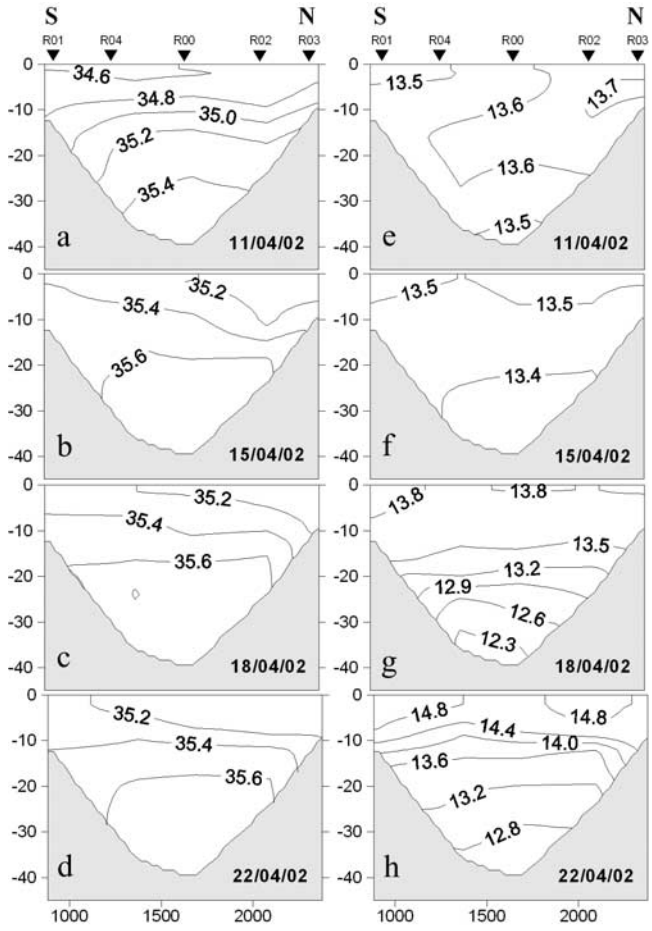

Figure 8. Contour plots of (a–d) salinity and (e–h) temperature along the section between Cabo de Mar and Punta Borneira from 11 to 22 April 2002.

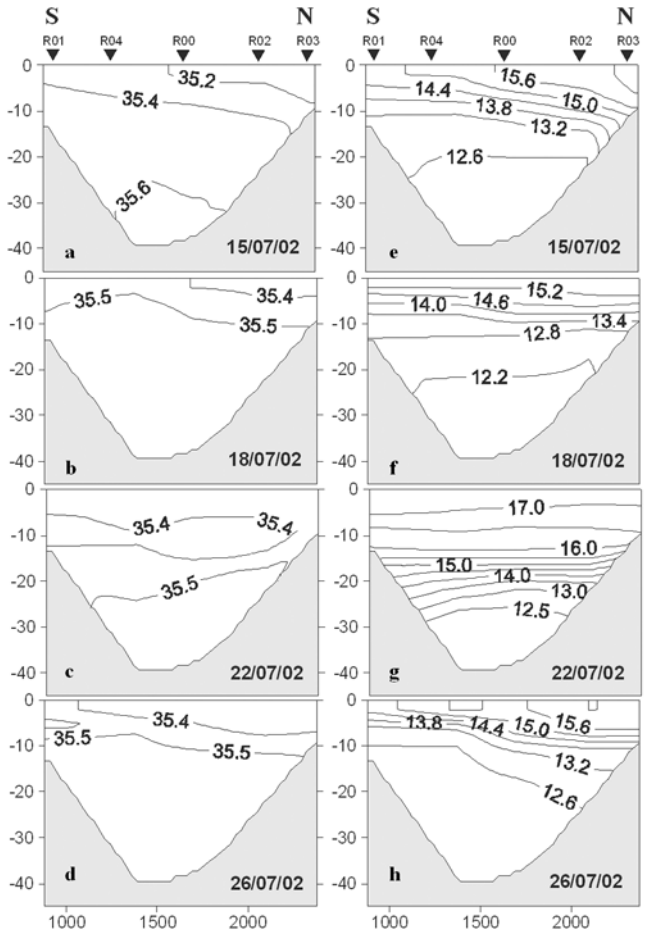

Figure 9. Contour plots of (a–d) salinity and (e–h) temperature along the section between Cabo de Mar and Punta Borneira from 15 to 26 July 2002.

(>17°C) and relatively salty (>34.8) shelf surface waters occupying the surface layer of the middle ría (Figures 10a and 10e). The persistence of shelf southerly winds produced a deepening of the surface salinity and temperature as a consequence of downwelling; bottom salinities were as low as 35.0 (Figures 10b and 10c) and bottom temperatures increased to 16°C (Figures 10f and 10g) from 17 to 23 September. Downwelling contributed to homogenize the salinity through the water column, but the solar irradiation was able to keep the temperature gradient. Southerly winds changed to northeasterly on 22 September, and this effect was recorded in the water column with a slight uplift of the isohalines (Figure 10d) and isotherms (Figure 10h), suggesting the entry of oceanic ENACW through the bottom layers on 26 September.

4. Discussion

[42] The sampling program allowed to capture the hydrographic (salinity and temperature distributions) and dynamic (residual circulation profiles) response of the water column over the wide range of (1) remote and local winds intensity and direction and (2) thermal and/or haline stratification/mixing conditions in a coastal upwelling embayment of the northwest Iberian coast. The winter period (February 2002) was characterized by a marked thermal inversion under an unexpectedly low continental runoff, as compared with a long-term average [*Nogueira et al.*, 1997]. Winds were very variable in magnitude and direction during the incipient stratification of the spring period (April 2002). During the summer period (July 2002), a succession of short-time upwelling events separated by intervals of stratification was recorded, a pattern typical of the upwelling season of coastal upwelling systems at temperate latitudes [*Álvarez-Salgado et al.*, 1993; *Hill et al.*, 1998]. Finally, during the autumn (September 2002), the pattern reversed, and short-time downwelling events, separated by intervals of stratification, were observed.

4.1. Remote Winds, a Key Forcing Agent of the Subtidal Motion in Estuaries and Coastal Inlets

[43] Since the middle 1970s the significance of shelf wind forcing in driving the motion in estuaries and bays has been recognized [*Carter et al.*, 1979]. In the last 2 decades, the effort concentrated on the wind-induced subtidal variability in partially mixed estuaries of diverse sizes, such as the San Francisco Bay [*Walters*, 1982; *Walters and Gartner*, 1985], the Delaware Bay [*Wong and Garvine*, 1984; *Wong and Moses-Hall*, 1998], and the Chesapeake Bay [*Vieira*, 1985, 1986; *Valle-Levinson*, 1995; *Valle-Levinson et al.*, 1998].

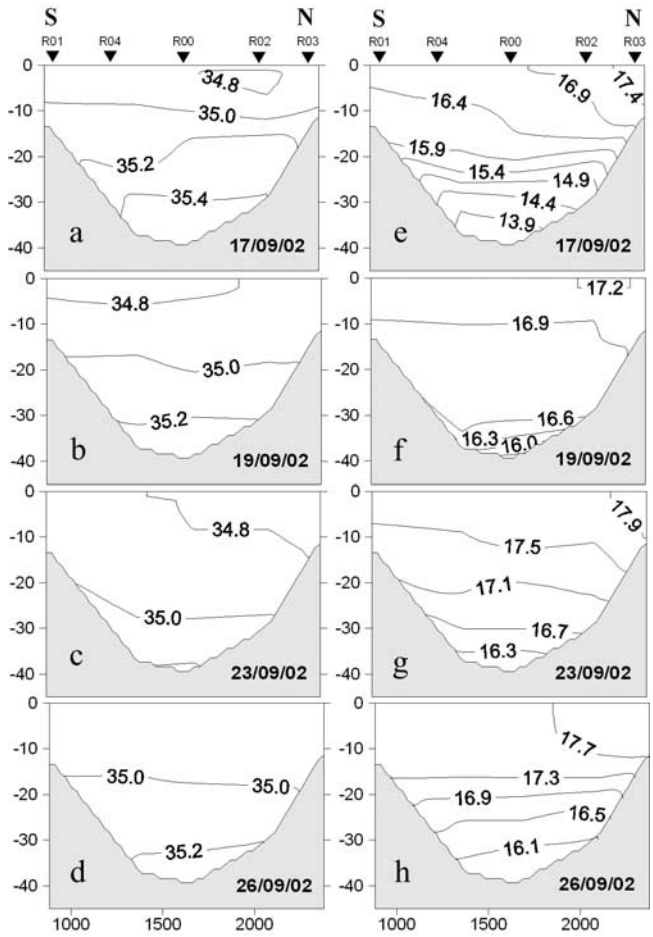

Figure 10. Contour plots of (a–d) salinity and (e–h) temperature along the section between Cabo de Mar and Punta Borneira from 17 to 26 September 2002.

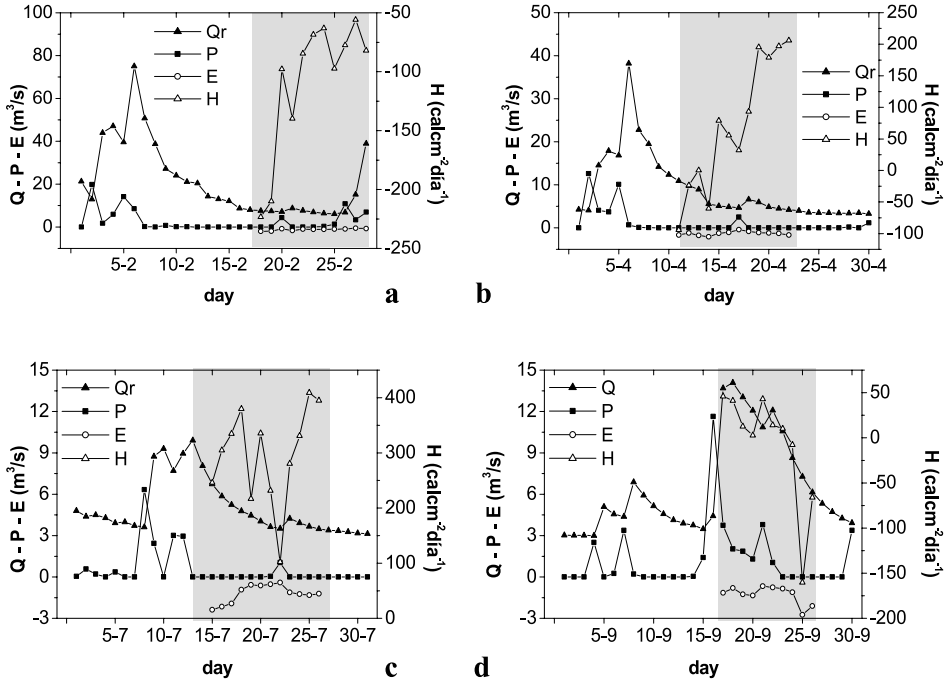

Figure 11. Hydrological balance terms: Q (continental runoff), P (precipitation), and E (evaporation) in $m^3\ s^{-1}$ (left axis) and radiative balance, H, in cal $cm^{-2}\ d^{-1}$ (right axis) for the (a) winter, (b) spring, (c) summer, and (d) autumn periods. The shaded areas indicate the sampling periods.

Furthermore, atmospheric forcing is also relevant for the subtidal variability in coastal lagoons with restricted communication with the ocean [e.g., *Wong and Wilson*, 1984; *Wong and DiLorenzo*, 1988]. These studies revealed that the subtidal variability in estuaries is mainly induced by winds, through a combination of remote and local effects.

[44] The effect of shelf winds is particularly relevant in an embayment affected by coastal upwelling. This is the case of the Rías Baixas in northwest Spain [*Rosón et al.*, 1997; *Álvarez-Salgado et al.*, 2000; *Pardo et al.*, 2001; *Gilcoto et al.*, 2001], Asysen Fjord in Southern Chile [*Cáceres et al.*, 2002], or Bantry Bay in South West Ireland [*Edwards et al.*, 1996].

[45] All these coastal inlets are located in temperate latitudes, where upwelling is not permanent but seasonal and repeated wind stress/relaxation cycles of period 1–2 weeks occur during the upwelling season [*Hill et al.*, 1998]. For the case of the northwest Iberian upwelling, a sampling strategy consisting on visiting the study site every 3–4 days was commonly applied during the 1990s to assess the response of the water column to the shelf wind stress/relaxation cycles [*Rosón et al.*, 1997; *Álvarez-Salgado et al.*, 2000; *Pardo et al.*, 2001]. These authors stated that at the timescale of the sampling frequency, the water column responded immediately to shelf wind stress. Later, *Gilcoto et al.* [2001] observed that the subtidal circulation of the surface layer of the Ría de Vigo was delayed less than one-half week compared with shelf winds, after analyzing the data obtained with a mechanic current meter deployed during a short period in September 1990. Therefore they demonstrated that a sampling frequency of 3–4 days was insufficient to study the lag time between subtidal circulation and shelf winds. Combination of continuous records of shelf winds and residual currents recorded at 10-min intervals in the present work allowed to quantify this lag time by means of a cross-correlation analyses. Lag times from 0 to 24 hours at 6-hour intervals were tested. Maximum correlation coefficients (>65%) between shelf winds and residual current

Table 2. Analysis of the Regression Between the Offshore Ekman Transport Calculated From Shelf Winds (Cabo Silleiro) and the Surface Flow Calculated With the DCM12 Current Meter Moored at Station R00 During February, July, and September for Time Lags of 0 to −24 Hours at −6-Hour Intervals[a]

Time Lag, hours	Slope, km	*y* Intercept, $m^3\ s^{-1}$	*R*	R^2
	February			
0	−2.3 ± 0.1	497 ± 72	−0.89	0.79
−6	−2.4 ± 0.1	552 ± 75	−0.89	0.79
−12	−2.4 ± 0.1	594 ± 91	−0.84	0.71
−18	−2.4 ± 0.1	624 ± 112	−0.77	0.59
−24	−2.4 ± 0.2	640 ± 133	−0.67	0.45
Average (0, −12)	−2.4 ± 0.1	569 ± 75	−0.89	0.79
	July			
0	−2.1 ± 0.1	1386 ± 124	−0.75	0.56
−6	−2.0 ± 0.1	1323 ± 111	−0.78	0.61
−12	−2.0 ± 0.1	1766 ± 119	−0.80	0.64
−18	−2.0 ± 0.1	1709 ± 116	−0.80	0.64
−24	−2.1 ± 0.1	1158 ± 116	−0.80	0.64
Average (0, −12)	−2.1 ± 0.1	1360 ± 11	−0.79	0.63
Average (0, −18)	−2.1 ± 0.1	1353 ± 106	−0.81	0.65
	September			
0	−2.6 ± 0.2	−233 ± 92	−0.75	0.56
−6	−2.6 ± 0.2	−261 ± 84	−0.80	0.63
−12	−2.5 ± 0.3	−296 ± 82	−0.80	0.63
−18	−2.4 ± 0.3	−332 ± 88	−0.77	0.59
−24	−2.3 ± 0.3	−369 ± 89	−0.77	0.59
Average (0, −12)	−2.6 ± 0.2	−308 ± 80	−0.81	0.65

[a]The 95% confidence intervals of the slope and *y* intercept are provided.

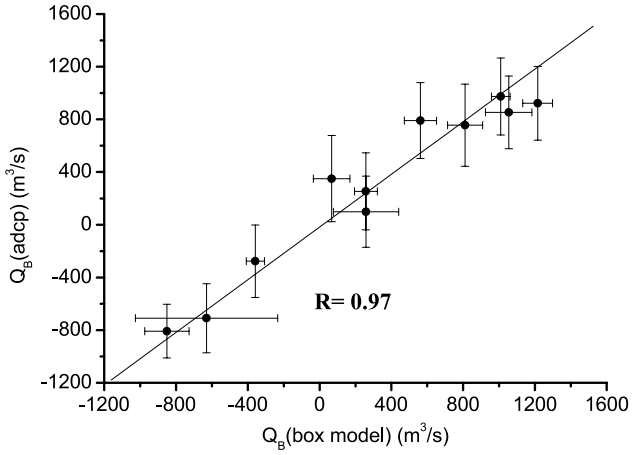

Figure 12. Linear regression between bottom water fluxes calculated with the inverse box model of *Álvarez-Salgado et al.* [2000] and the measurements preformed with the DCM12 current meter.

records were obtained for lag times of 12 hours in February and September. In July, the correlation coefficient was not different for shelf winds blowing over the last 24 hours (Table 2). The short lag times observed in the Ría de Vigo are probably related to the relatively small size of the rías compared with other embayments. In this sense, the small size of San Francisco Bay was the reason argued by *Walters* [1982] to explain the higher-frequency response in comparison with the much larger Chesapeake Bay. *Wong* [2002] found that remote wind-induced coastal pumping effect is by far the most important mechanism to force the subtidal current fluctuations in Chesapeake Bay over timescales of 2–3 days. The percentage of the observed subtidal current variability explained by shelf winds in the Ría de Vigo (>65%) was much larger than the 25% found in the Potomac Estuary by *Elliott* [1978] and of the same order of the 70% found in the Chesapeake Bay by *Wong* [2002].

[46] A model II linear regression analysis [*Sokal and Rohlf*, 1994] was applied to the offshore Ekman transport ($m^3\ s^{-1}\ km^{-1}$) calculated from shelf winds and the surface fluxes ($m^3\ s^{-1}$) recorded at station R00 with the ADCP current meter. The results are presented in Table 2 for the winter, summer, and autumn periods. The slopes of the regression lines are comparable with the wideness of the surface layer of the middle Ría de Vigo (2.2 km). This observation indicates that the middle ría is under the direct influence of shelf wind stress. A similar result was obtained by *Rosón et al.* [1997] in the Ría de Arousa and *Álvarez-Salgado et al.* [2000] in the Ría de Vigo, with their inverse method. It should be noted again that the results of an inverse method are applicable to the timescale of a sampling frequency (one-half week) that largely exceed the lag time of response of the rías to shelf winds. However, the results of the direct and continuous measurements of this work indicate that the ría behaves as an extension of the shelf at the short timescale of the lag time.

[47] The *y* intercept of the regression equations in Table 2 represents the intrinsic circulation of the ría after removal of the variability due to shelf winds. A positive *y* intercept indicates a negative intrinsic circulation (surface inflow), and a negative value indicates a positive intrinsic circulation (surface outflow). In view of these results, a negative intrinsic circulation was found in July and February, while in September it was positive.

[48] Although the two-layered residual circulation scheme is the most common in the Ría de Vigo, a three-layered residual circulation develops under the influence of low-intensity shelf winds during the transition from upwelling to downwelling-favorable conditions and vice versa. It consists of an outflow through the surface and bottom and an inflow through the intermediate layer. *Álvarez-Salgado et al.* [1998] detected the same pattern during a 1-day period in September 1991 in the Ría de Vigo. This pattern has also been found by *Valle-Levinson et al.* [2002] studying the effect of winds on the exchange flow of a channel constriction of the Chilean Inland Sea. They found a three-layer response to winds that opposed the density-induced near-surface outflow and corresponded with other observations [*Svendsen and Thomson*, 1978; *Cáceres et al.*, 2002] and numerical simulations [*Klinck et al.*, 1981] in other systems. The circulation pattern of an archetypal fjord also consists of three layers: a surface layer, flowing seaward, driven by river discharge at the head of the fjord; an intermediate layer, flowing landward; and a deep layer, which is only replaced when the intermediate inflow is sufficiently dense to displace the existing deep water. Although the morphology and origin of the rías are different from fjords, they have analogous characteristics. In fact, wind forcing can be the main driving mechanism in both systems, and the two systems present evidences of wind-induced upwelling; Aysen Fjord, on the southern coast of Chile [*Cáceres et al.*, 2002], presented a three-layer structure that was consistent with up-fjord wind-

Table 3. Time Evolution of the Bottom Flow in the Middle Segment of the Ría de Vigo, $\overline{Q}_B$, Between Two Consecutive Surveys During the Four Study Periods as Calculated With the Inverse Method of *Álvarez-Salgado et al.* [2000][a]

Days	$(Q_B)_R$, m^3/s	$(Q_B)_H$, m^3/s	$(Q_B)_{NSS}$, m^3/s	Q_B, m^3/s
		February		
18/21	572	136	346	1054
21/25	599	77	−608	67
25/28	94	2533	−3257	−630
		April		
11/15	471	−1	1496	1967
15/18	442	108	260	811
18/22	199	300	−240	258
		July		
15/18	61	628	526	1215
18/22	24	436	−819	−358
22/26	16	442	550	1009
		September		
17/19	691	71	−1614	−851
19/23	1009	40	−790	259
23/26	274	−183	471	562

[a]The hydrological, $(Q_B)_H$, radiative, $(Q_B)_R$, and nonsteady-state term, $(Q_B)_{NSS}$ are separated.

induced exchange. The three-layered circulation could be understood as a transitional adjustment of the system to the dominant two-layered circulation commonly found in the Ría de Vigo.

4.2. Coupling Between Hydrography and Hydrodynamics

[49] In the present work, residual flows in the middle Ría de Vigo have also been assessed from the short-timescale variability of the distributions of salinity and temperature by means of the inverse method described in section 2.3. Simultaneous ADCP measurements allowed comparison of two independent methods for calculating water flows. Figure 12 presents the relationship between measured (ADCP) and calculated (inverse method) water flows. The 1:1 line explained 94% of the variability of the calculated flows. Therefore both methods corroborate the validity of the calculated water fluxes. *Gilcoto et al.* [2001] obtained the first comparison between measured and calculated flows, matching the output of an inverse method and the surface residual currents obtained with a mechanic current meter deployed at 3 m depth in the central Ría de Vigo. However, *Gilcoto et al.*'s [2001] data reduce to just four observations during a 2-week period in September 1990.

[50] Water displacements evaluated from direct current measurements are restricted to the mooring position, a single depth in the case of the mechanic current meter of *Gilcoto et al.* [2001], while the inverse method extended to the complete cross section. Furthermore, the possibility of splitting the residual fluxes calculated with the inverse method into three terms allows assessment of their relative contribution to the total residual flow. Table 3 shows (1) the time evolution of the bottom water flux in the middle ría, $\overline{Q}_B$, calculated with the inverse method; (2) the nonsteady-state term of $\overline{Q}_B$, $\left(\overline{Q}_B\right)_{NSS}$; and (3) the steady-state term of $\overline{Q}_B$, divided into a hydrological term, $\left(\left(\overline{Q}_B\right)_{SS}\right)_H$, and a radiative term, $\left(\left(\overline{Q}_B\right)_{SS}\right)_R$. An analysis of the variance of the three terms (σ^2_{NSS}, σ^2_{H}, and σ^2_{R}) yielded that the short-timescale evolution of $\overline{Q}_B$ was primarily controlled by the nonsteady-state term (72% of $\sigma^2_{\mathrm{NSS}} + \sigma^2_{\mathrm{H}} + \sigma^2_{\mathrm{R}}$), then by the radiative term (24%) and, residually by the hydrological term (4%).

[51] The nonsteady-state term, which depended on the temporal changes in salinity ($\Delta S/\Delta t$) and temperature ($\Delta T/\Delta t$), correlated significantly with the offshore Ekman transport, $-\overline{Q}_X$, considering the 16 pairs of data obtained by *Álvarez-Salgado et al.* [2000] combined with the 12 pairs obtained in this work,

$$\left(\overline{Q}_B\right)_{NSS} = 284(\pm 56) - 0.37(\pm 0.05)\overline{Q}_X$$
$$R = -0.83, n = 28, p < 0.0001 \tag{23}$$

In view of these results, about 70% of the variability in the bottom flow, at the timescale of the sampling frequency (one-half week), depended on the nonsteady-state term, and the offshore Ekman transport controlled 70% of the variability of the nonsteady-state term.

[52] In addition, combing the data of surface water flows, $\overline{Q}_S$, continental runoff, $\overline{Q}_R$, and offshore Ekman transport, $-\overline{Q}_X$, obtained by *Álvarez-Salgado et al.* [2000] from 1990 to 1997, with the terms obtained in this work, produced the following empirical equation:

$$\overline{Q}_S = 13(\pm 4)10^{-3}\overline{Q}_R - 2.2(\pm 0.2)10^{-3}\overline{Q}_X$$
$$R = 0.92, n = 27, p < 0.001. \tag{24}$$

The regression coefficients of equation (24) are not significantly different from those obtained by *Álvarez-Salgado et al.* [2000], indicating that the 2002 data were consistent with the previous fit. Note that the coefficient of $-Q_X$, 2.2 ± 0.2 km, is again comparable with the wideness of the surface layer of the middle Ría de Vigo.

[53] A second way to compare the results obtained from direct measurements and inverse method calculations is the depth of the level of no motion (LNM) between the outgoing (ingoing) surface current and the outgoing (ingoing) bottom current obtained with both methods. Traditionally, the LNM in box models was set at the depth of the halocline [*Pritchard*, 1952; *Officer*, 1980]. In the case of the Rías Baixas, since both the salinity and temperature profiles are considered, the LNM has been preferentially set at the pycnocline [*Rosón et al.*, 1997; *Álvarez-Salgado et al.*, 2000; *Gilcoto et al.*, 2001; *Pardo et al.*, 2001]. In this work, this hypothesis has been corroborated: The difference between the two sets of LNM depths was 0 ± 2.5 m.

[54] A significant transversal variability was found in the salinity and temperature distributions of the middle segment of the Ría de Vigo. In general, the northern margin was fresher and warmer than the southern margin of the ría. This gradient is caused by the Coriolis deflection of continental waters under a positive residual circulation pattern. The same reason is applicable to the entry of the cold and salty ENACW through the southern bottom margin. In addition, the 3-D residual circulation pattern of the outer ría [*Souto et al.*, 2003] seems to play a significant role in the asymmetry of the residual currents in the middle ría [*Gilcoto*, 2004] and therefore in the transversal variability of the thermohaline properties.

[55] Finally, an additional source of variability of the thermohaline structure of the middle ría is the quality of the ENACW upwelled over the northwest Iberian shelf that enters the ría: It was warmer and saltier in winter (>35.8) than in summer (<35.6) The Galician Rías Baixas are located at the boundary between the temperate and subpolar regimes of the eastern North Atlantic, where two branches of ENACW can upwell. These two branches were described first by *Fraga et al.* [1982], who observed that they meet in a quasi permanent subsurface front that migrates seasonally from south of River Miño in winter to east of River Eo in summer (Figure 1) according to *Castro* [1997]. *Ríos et al.* [1992a] characterized the origin of both branches: (1) ENACW of subpolar origin (ENACWp) represents the water bodies formed to the north of Cabo Fisterra, and (2) ENACW of subtropical origin (ENACWt) formed to the south of Cape Roca. These authors established that ENACWt has a salinity >35.66 and ENACWp <35.66. During the downwelling season, warm and saltier surface waters of subtropical origin are promoted by the Iberian Poleward Current off the Rías Baixas [*Haynes and Barton*, 1990, 1991]. They pile on the shelf and enter the rías through the surface or bottom layer depending on shelf

winds. Therefore the origin of upwelled water into the rías depends on (1) the seasonal migration of the front and (2) the vertical displacements of ENACW promoted by the shelf winds: Northerly winds of high intensity produce the entry of the deeper ENACWp branches into the ría during the summer. A similar subsurface front between water masses is found off Cape Blanco, northwest Africa (21°N). South of the cape, SACW (South Atlantic Central Water) upwells, with lower salinity and higher nutrient concentrations than the NACW (North Atlantic Central Water) that upwells north of the cape [*Fraga et al.*, 1985].

5. Conclusions

[56] Although the basic knowledge on the hydrodynamics of the Spanish Rías Baixas developed over the last decade with inverse models based on hydrographic data, direct current measurements are still scarce, with a poor spatial and temporal coverage. This study was specifically designed to analyze the short time and space scale variability of the hydrodynamics of the Ría de Vigo, the paradigm of a coastal embayment under the influence of coastal upwelling, from an intensive recording program of the vertical structure and displacements of the water column.

[57] The following conclusions can be drawn.

[58] 1. Remote shelf winds controlled more than 65% of the variability observed in the subtidal circulation of the ría, whereas the heat exchange with atmosphere represented less than 25% and continental runoff represented less than 5% at an annual basis. Local winds did not contributed significantly to the subtidal circulation of the ría.

[59] 2. The subtidal circulation of the ría responded to the effect of shelf wind with an average lag time ranging from 0 to 2 days, depending on the layer and the time of the year. Commonly, the lag is less than 1 day. This rapid response compared with other estuaries and coastal embayments is probably related to the comparatively small size of the ría and the V-shaped topography.

[60] 3. The two-layered residual circulation pattern, assumed with the inverse models and calculated with the numeric models of the Ría de Vigo, has been confirmed by repetitive measurements in the central part of the embayment under contrasting hydrographic and meteorological conditions. In addition, a three-layered circulation pattern has been identified during the transition from positive to negative circulation and vice versa.

[61] **Acknowledgments.** The authors wish to thank the captain, crew, and technicians of R/V *Mytilus* as well as the Group of Physical Oceanography of the University of Vigo and the Group of Oceanography of the Instituto de Investigacións Mariñas (CSIC) for their collaboration during the sampling program. Special thanks are owed to P. C. Pardo and M. Gilcoto for their comments and suggestions. We are also grateful to E. A. Fanjul and B. Morón for the meteorological data of the Silleiro buoy. S. P. and J. L. H. have been funded by FPI fellowships of the Spanish Ministerio de Educación y Ciencia. Financial support for this work came from the Spanish Ministerio de Educación y Ciencia, grant REN2000-0880-C02-01 MAR and the Xunta de Galicia grant PGIDT01MAR40201PN. This is contribution 26 of the Unidad Asociada CSIC-GOFUVI.

References

Agsterberg, R., and J. Wieringa (1989), Mesoscale terrain roughness mapping of the Netherlands, *Tech. Rep. TR-115*, R. Netherlands Meteorol. Inst., De Bilt, Netherlands.

Álvarez-Salgado, X. A., G. Rosón, F. F. Pérez, and Y. Pazos (1993), Hydrographic variability off the Rías Baixas (NW Spain) during the upwelling season, *J. Geophys. Res.*, *98*, 14,447–14,455.

Álvarez-Salgado, X. A., F. G. Figueras, M. L. Villarino, and Y. Pazos (1998), Hydrodynamic and chemical conditions during onset of a red-tide assemblage in an estuarine upwelling ecosystem, *Mar. Biol.*, *130*, 509–519.

Álvarez-Salgado, X. A., J. Gago, B. M. Miguel, M. Gilcoto, and F. F. Pérez (2000), Surface waters of the NW Iberian Margin: Upwelling on the shelf versus outwelling of upwelled waters from the Rías Baixas, *Estuarine Coastal Shelf Sci.*, *51*, 821–837.

Bakun, A., and C. S. Nelson (1991), The seasonal cycle of wind-stress curl in subtropical eastern boundary current regions, *J. Phys. Oceanogr.*, *21*, 1815–1834.

Cáceres, M., A. Valle-Levinson, H. H. Sepúlveda, and K. Holderied (2002), Transverse variability of flow and density in a Chilean fjord, *Cont. Shelf Res.*, *22*, 1683–1698.

Carter, H. H., T. O. Najarian, D. W. Pritchard, and R. E. Wilson (1979), The dynamics of motion in estuaries and other coastal water bodies, *Rev. Geophys.*, *17*(7), 1585–1590.

Castro, C. G. (1997), Caracterización química del agua subsuperficial del Atlántico Nororiental y su modificación por procesos biogeoquímicos, Ph.D. dissertation, 244 pp., Univ. of Santiago, Santiago de Compostela, Spain.

Edwards, A., K. Jones, J. M. Graham, C. R. Griffiths, N. MacDougall, J. Patching, J. M. Patching, J. M. Richard, and R. Raine (1996), Transient coastal upwelling and water circulation in Bantry Bay, a ría on the southwest coast of Ireland, *Estuarine Coastal Shelf Sci.*, *42*, 213–230.

Elliott, A. J. (1978), Observations of the meteorologically induced circulation in the Potomac Estuary, *Estuarine Coastal Mar. Sci.*, *6*, 285–290.

Figueiras, F. G., U. Labarta, and M. J. Fernández Reiriz (2002), Coastal upwelling, primary production and mussel growth in the Rías Baixas of Galicia, *Hydrobiologia*, *484*, 121–131.

Fraga, F. (1981), Upwelling off the Galician coast, northwest Spain, in *Coastal Upwelling*, *Coastal Estuarine Sci.*, vol. 1, edited by F. A. Richards, pp. 176–182, AGU, Washington, D. C.

Fraga, F., C. Mouriño, and M. Manríquez (1982), Las masas de agua en la costa de Galicia: Junio–Octubre, *Res. Exped. Cient.*, *10*, 51–77.

Fraga, F., E. D. Barton, and O. Llinas (1985), The concentration of nutrient salts in "pure" North and South Atlantic central waters, *Invest. Pesq.*, *5*(1), 25–36.

Gilcoto, M. (2004), El campo termohalino como trazador de la dinámica de la Ría de Vigo y su acoplamiento meteorológico, Ph.D. dissertation, 211 pp., Univ. of Vigo, Vigo, Spain.

Gilcoto, M., X. A. Álvarez Salgado, and F. F. Pérez (2001), Computing optimum estuarine residual fluxes with a multiparameter inverse model method (OERFIM): Application to the Ría de Vigo (NW Spain), *J. Geophys. Res.*, *106*, 31,303–31,318.

Gill, A. E. (1982), *Atmosphere-Ocean Dynamics*, *Int. Geophys. Ser.*, vol. 30, edited by W. L. Donn, Elsevier, New York.

Godin, G. (1972), *The Analysis of Tides*, Liverpool Univ. Press, Liverpool, UK.

Haynes, R., and E. D. Barton (1990), A poleward flow along the Atlantic coast of the Iberian Peninsula, *J. Geophys. Res.*, *95*, 11,425–11,441.

Haynes, R., and E. D. Barton (1991), Lagrangian observations in the Iberian Coastal Transition Zone J, *J. Geophys. Res.*, *96*, 14,731–14,741.

Hidy, G. M. (1972), A view of recent air-sea interaction research, *Bull. Am. Meteorol. Soc.*, *53*, 1083–1102.

Hill, A. E., B. M. Hickey, F. A. Shillington, P. T. Strub, K. H. Brink, E. D. Barton, and A. C. Thomas (1998), Eastern ocean boundaries coastal segment (E), in *The Sea*, vol. 11, edited by A. R. Robinson and K. H. Brink, pp. 29–67, John Wiley, Hoboken, N. J.

Kelly, K. A., G. S. E. Lagerloef, and R. L. Bernstein (1988), Comment on "Empirical orthogonal function analysis of Advanced very high resolution radiometer surface temperature patterns in the Santa Barbara channel," *J. Geophys. Res.*, *93*, 15,752–15,754.

Klinck, J., J. O'Brien, and H. Svendsen (1981), A simple model of fjord and coastal circulation interaction, *J. Phys. Oceanogr.*, *11*, 1612–1626.

Kundu, P. K., and J. S. Allen (1976), Some three-dimensional characteristics of low frequency current fluctuations near the Oregon coast, *J. Phys. Oceanogr.*, *6*, 181–199.

Laevastu, T. (1963), Energy exchange in the North Pacific, its relations to weather and its oceanographic consequences: 1. Formulas and monograms for computation of heat exchange components over the sea, *Rep. 29:15*, Hawaiian Inst. of Geophys., Honolulu.

Míguez, B. M., F. F. Pérez, C. Souto, and L. Fariña-Busto (2001), Flujos residuales de intercambio entre la Ría de Vigo y la plataforma continental, *Fís. Tierra*, *13*, 119–137.

Nogueira, E., F. F. Pérez, and A. F. Ríos (1997), Seasonal and long-term trends in an estuarine upwelling ecosystem (Ría de Vigo, NW Spain), *Estuarine Coastal Shelf Sci.*, *44*, 285–300.

Officer, C. B. (1980), Box models revisited, in *Estuarine and Wetlands Processes With Emphasis on Modelling*, edited by P. Hamilton and K. B. McDonald, pp. 65–114, Springer, New York.

Otto, L. (1975), Oceanography of the Ría de Arousa (NW Spain), *Rep. 96*, 210 pp., R. Neth. Meteorol. Inst. (KNMI), De Bilt, Netherlands.

Pardo, P. C., M. Gilcoto, and F. F. Pérez (2001), Short-time scale coupling between thermohaline and meteorological forcing in the Ría de Pontevedra, *Sci. Mar.*, *65*, Suppl. 1., 229–240.

Pritchard, D. W. (1952), Salinity distribution and circulation in the Chesapeake Bay estuarine system, *J. Mar. Res.*, *11*, 106–123.

Pritchard, D. W. (1956), The dynamic structure of a coastal plain estuary, *J. Mar. Res.*, *15*, 33–42.

Ríos, A. F., F. F. Pérez, and F. Fraga (1992a), Water masses in upper and middle North Atlantic Ocean east of Azores, *Deep Sea Res.*, *39*, 645–658.

Ríos, A. F., M. A. Nombela, F. F. Pérez, G. Rosón, and F. Fraga (1992b), Calculation of runoff to an estuary, Ría de Vigo, *Sci. Mar.*, *56*, 29–33.

Rosón, G., X. A. Álvarez-Salgado, and F. F. Pérez (1997), A non stationary box model to determine residual fluxes in a partially mixed estuary, based on both thermohaline properties: Application to the Ria de Arousa (NW Spain), *Estuarine Coastal Shelf Sci.*, *44*, 249–262.

Schroeder, W. W., and W. J. Wiseman (1986), Low frequency shelf-estuarine exchange processes in Mobile Bay and other estuarine systems on the northern Gulf of Mexico, in *Estuarine Variability*, edited by D. A. Wolfe, pp. 355–367, Elsevier, New York.

Sokal, R. R., and F. J. Rohlf (1994), *Biometry: The Principles and Practice of Statistics in Biological Research*, W. H. Freeman, New York.

Souto, C., L. Fariña, E. Álvarez, and I. Rodríguez (2001), Wind and tide current prediction using a 3D finite difference model in the Ría de Vigo (NW Spain), *Sci. Mar.*, *65*, 269–276.

Souto, C., M. Gilcoto, L. Fariña-Busto, and F. F. Pérez (2003), Modeling the residual circulation of a coastal embayment affected by wind-driven upwelling: Circulation of the Ría de Vigo (NW Spain), *J. Geophys. Res.*, *108*(C11), 3340, doi:10.1029/2002JC001512.

Svendsen, H., and R. Thomson (1978), Wind driven circulation in a fjord, *J. Phys. Oceanogr.*, *8*, 703–713.

Torres-López, S., R. A. Varela, and E. Delhez (2001), Residual circulation and thermohaline distribution of the Ría de Vigo: A 3-D hydrodynamic model, *Sci. Mar.*, *65*, 277–289.

Valle-Levinson, A. (1995), Observations of barotropic and baroclinic exchanges in the lower Chesapeake Bay, *Cont. Shelf Res.*, *15*, 1631–1647.

Valle-Levinson, A., C. Li, T. Royer, and L. Atkinson (1998), Flow patterns at the Chesapeake Bay entrance, *Cont. Shelf Res.*, *18*, 1157–1177.

Valle-Levinson, A., J. L. Blanco, and J. J. Fierro (2002), Observations of wind effects on exchange flows in a channel constriction of the Chilean Inland Sea, paper presented at 2nd Meeting on the Physical Oceanography of Sea Straits, Off. of Naval Res., Villefranche, France.

Vieira, M. E. C. (1985), Estimates of subtidal volume flux in mid Chesapeake Bay, *Estuarine Coastal Shelf Sci.*, *21*, 411–427.

Vieira, M. E. C. (1986), The meteorologically driven circulation in mid-Chesapeake Bay, *J. Mar. Res.*, *44*, 473–493.

Walters, R. A. (1982), Low-frequency variations in sea level and currents in South Francisco Bay, *J. Phys. Oceanogr.*, *12*, 658–668.

Walters, R. A., and J. W. Gartner (1985), Subtidal sea level and current variations in the northern reach of San Francisco Bay, *Estuarine Coastal Shelf Sci.*, *21*, 17–32.

Wang, J. D., and A. J. Elliott (1978), Non-tidal variability in the Chesapeake Bay in the Potomac River: Evidence for non-local forcing, *J. Phys. Oceanogr.*, *8*, 225–232.

Weisberg, R. H. (1976), A note on estuarine mean flow estimation, *J. Mar. Res.*, *34*, 387–394.

Weisberg, R. H., and W. Sturges (1976), Velocity observations in the West Passage of Narragansett Bay: A partially mixed estuary, *J. Phys. Oceanogr.*, *6*, 345–354.

Wieringa, J. (1986), Roughness dependent geographical interpolation of surface winds speed averages, *Q. J. R. Meteorol. Soc.*, *112*, 867–889.

Wong, K. C. (2002), On the spatial structure of currents across the Chesapeake and Delaware Canal, *Estuaries*, *4A*, 519–527.

Wong, K. C., and J. DiLorenzo (1988), The response of Delaware's inland bays to ocean forcing, *J. Geophys. Res.*, *93*, 12,525–12,535.

Wong, K. C., and R. W. Garvine (1984), Observations of wind-induced, subtidal variability in the Delaware Estuary, *J. Geophys. Res.*, *89*, 10,589–10,597.

Wong, K. C., and J. E. Moses-Hall (1998), The tidal and subtidal variations in the transverse salinity and current distributions across a coastal plain estuary, *J. Mar. Res.*, *56*, 489–517.

Wong, K. C., and R. E. Wilson (1984), Observations of low-frequency variability in Great South Bay and relations to atmospheric forcing, *J. Phys. Oceanogr.*, *14*, 1893–1900.

Wooster, W. S., A. Bakun, and D. R. Mclain (1976), The seasonal upwelling cycle along the eastern boundary of the North Atlantic, *J. Mar. Res.*, *34*, 131–141.

X. A. Álvarez-Salgado, Instituto de Investigacións Mariñas, Consejo Superior de Investigaciones Científicas, Eduardo Cabello 6, E-36208 Vigo, Spain.

J. L. Herrera, S. Piedracoba, and G. Rosón, Universidade de Vigo, F. de Ciencias do Mar. Marcosende, E-36200 Vigo, Spain. (spiedra@uvigo.es)